

---

• RESEARCH PAPER •

# Topology-Driven Quantum Architecture Search Framework

Junjian Su<sup>1,2,3</sup>, Jiacheng Fan<sup>1</sup>, Shengyao Wu<sup>1</sup>, Guanghui Li<sup>1</sup>, Sujuan Qin<sup>1</sup> & Fei Gao<sup>1\*</sup>

<sup>1</sup>State Key Laboratory of Networking and Switching Technology, Beijing University of Posts and Telecommunications, Beijing 100876, china;

<sup>2</sup>National Engineering Research Center of Disaster Backup and Recovery, Beijing University of Posts and Telecommunications, Beijing 100876, china;

<sup>3</sup>School of Cyberspace Security, Beijing University of Posts and Telecommunications, Beijing 100876, china

---

**Abstract** The limitations of Noisy Intermediate-Scale Quantum (NISQ) devices have spurred the development of Variational Quantum Algorithms (VQAs), which hold the potential to achieve quantum advantage for specific tasks. Quantum Architecture Search (QAS) algorithms are pivotal in automating the design of high-performance Parameterized Quantum Circuits (PQCs) for VQAs. However, existing QAS algorithms grapple with excessively large search spaces, resulting in significant computational complexity when searching large-scale quantum circuits. To address this challenge, we propose a Topology-Driven Quantum Architecture Search (TD-QAS) framework. Our framework initially employs QAS to identify optimal circuit topologies and subsequently utilizes an efficient QAS to fine-tune gate types. In the fine-tuning phase, the QAS inherits parameters from the topology search phase, thereby eliminating the need to train from scratch. By decoupling the extensive search space into topology and gate-type components, TD-QAS avoids exploring gate configurations within low-performance topologies, significantly reducing computational complexity. Numerical simulations across various tasks, under both noiseless and noisy scenarios, demonstrate that the TD-QAS framework enhances the efficiency of QAS algorithms by enabling them to identify high-performance quantum circuits with lower computational complexity. These results suggest that TD-QAS will deepen our understanding of VQA and have broad applicability in future QAS algorithms.

**Keywords** Quantum machine learning, Variational quantum algorithm, Quantum variational circuits, Quantum architecture search, Search space decoupling

---

**Citation** Topology-Driven Quantum Architecture Search Framework. , for review

---

## 1 Introduction

Quantum computing exhibits promising potential in addressing complex problems such as combinatorial optimization [1,2], factoring [3], linear system solving [4], chemical simulations [5], and machine learning [6–12]. However, Noisy Intermediate-Scale Quantum (NISQ) devices [13], representing the cutting edge of near-term quantum technology, encounter significant challenges, including noise, a limited number of qubits, and restricted qubit connectivity. These limitations impede the widespread application of quantum computing [14]. To mitigate these issues, Variational Quantum Algorithms (VQAs) have been developed to operate within the constraints of NISQ devices [15–18], offering the potential to achieve quantum advantage for specific tasks.

A critical factor in the effectiveness of VQAs is the design of Parameterized Quantum Circuits (PQCs) [19,20]. Quantum Architecture Search (QAS) is a technique for automating the search for high-performing PQCs [21–30]. QAS aim to explore the optimal quantum circuit in a vast search space encompassing all possible circuit configurations. Consequently, QAS algorithms face the challenge of excessive computational complexity due to the need to explore an exponentially large search space, particularly when targeting large-scale quantum circuits [31]. Therefore, developing methods to efficiently reduce the search space is essential for enhancing the efficiency and scalability of QAS.

Quite a few methods have already been proposed to reduce the search space for QAS algorithms. A common strategy involves imposing rigid constraints on PQC design [32], such as restricting quantum gates to operate only on fixed qubits rather than arbitrary qubits. However, these methods indiscriminately discard a large number of potential PQCs without any targeted strategy, which may inadvertently

---

\* Corresponding author (email: gaof@bupt.edu.cn)

eliminate optimal circuit. Another approach focuses on identifying components of quantum circuits and constructing larger circuits by repeating these components [27, 33]. This method is particularly suitable for managing large search spaces, although it may result in circuits with greater depth. Additionally, a preprocessing method has been proposed for QAS to eliminate low-performance quantum circuits [34]. While this method significantly improves the search efficiency of QAS, they introduce additional computational complexity.

In this paper, we propose a novel framework to significantly reduce the search space in QAS. Our approach is inspired by Neural Architecture Search (NAS), which aims to automatically discover high-performance neural network architectures for a given task [36]. It is well established that the performance of Convolutional Neural Networks (CNNs) identified through NAS remains relatively robust to the random replacement of specific operations [37]. Building on this observation, we consider whether a similar phenomenon could be observed in VQA, where topology plays a more crucial role than specific gate types in determining performance. This motivates us to investigate a method of decoupling the QAS process into two independent components, i.e., topology and gate types. The decoupling method enables QAS to avoid exploring gate-type configurations associated with low-performance topologies.

Through extensive numerical simulations, detailed in Section 4.1, we validate that topology indeed plays a dominant role over gate types in the search for high-performance quantum circuits. This finding suggests that by fixing the gate types and concentrating solely on topology, QAS can effectively identify high-performance quantum circuits. Furthermore, we observe that during the gate-type optimization phase, the trainable parameters of QAS can be inherited from the topology search phase. This inheritance eliminates the need for training from scratch, thereby accelerating convergence. Consequently, we propose the Topology-Driven Quantum Architecture Search (TD-QAS) framework, which prioritizes an independent search for high-performance topologies followed by an efficient fine-tuning of gate types. The TD-QAS framework effectively decouples the original search space into two distinct spaces, i.e., topology and gate types, thereby significantly reducing the overall search space. We conducted numerical simulations across a variety of tasks in both noiseless and noisy scenarios. These results demonstrate that the proposed TD-QAS framework enables QAS algorithms to identify quantum circuits with comparable performance while maintaining significantly low computational complexity, compared by original QAS algorithms that searching both topology and gate types. This study not only deepens our understanding of VQAs but also significantly extends the applicability of QAS to more complex tasks, paving the way for more efficient and scalable approaches to designing quantum circuits.

## 2 Background and Related Work

### 2.1 Quantum Architecture Search

QAS is a promising technique for automating the search of high-performing PQCs, capable of integrating specific target tasks or additional constraints during the search process [30]. It navigates the vast search space of potential quantum circuits by employing a search strategy to generate candidate circuits, followed by an evaluation strategy to assess their performance. The feedback from these performance is then used to optimize the search model’s trainable parameters. However, QAS faces significant challenges related to high computational complexity, prompting the development of various approaches to mitigate these expenses.

Efforts to reduce the computational complexity of QAS have concentrated on three key aspects: search strategy, evaluation strategy, and search space optimization. **Search Strategy:** The most basic search strategy is a random search method, which often demands an impractically large number of iterations to locate an effective circuit, leading to excessive computational complexity. To address this challenge, more sophisticated search models have been introduced to enhance search efficiency or reduce training costs. These advanced models include evolutionary algorithms, reinforcement learning [21], differentiable algorithms [24], Bayesian optimization methods [27], and so on. **Evaluation Strategy:** While these methods are effective in improving search efficiency, they necessitate substantial feedback for parameter training, resulting in the evaluation of an excessive number of quantum circuits. To mitigate the high computational burden associated with evaluating numerous quantum circuits, more efficient evaluation techniques have been developed. These methods aim to accelerate the evaluation process while striving to maintain evaluation accuracy. Notable approaches include shared parameter evaluation (one-shot techniques) [23], performance predictor-based evaluations [25], and training-free predictors [28]. **Search Space Optimization:** The extensive search space in QAS introduces additional challenges, not only in terms of the search model’s ability to efficiently learn from the exploration process but also in accurately evaluating the performance of quantum circuits. To overcome these obstacles, various techniques have been proposed to reduce the search space. These include imposing strict constraints on quantum gate operations [31], searching for small-scale circuit components to build larger circuits [27, 32], and employing search space pruning method [33]. By narrowing down the search space, these techniques enhance the efficiency and scalability of QAS, enabling it to focus on more promising regions of the search space.

In this work, we implement the TD-QAS framework using two representative QAS algorithms, i.e., QuantumSupernet [23] and DQAS [24], to validate the improvements brought by our framework over traditional QAS algorithms. The following subsections provide detailed introductions to these two algorithms.

#### 2.1.1 *QuantumSupernet*

QuantumSupernet, proposed by Du et al. [23], is an advanced QAS algorithm designed to optimize the search process for high-performing quantum circuits. We introduce the QuantumSupernet by focusing on three QAS’s key aspects. QuantumSupernet employs a supernet to define the search space, which is composed of multiple layers containing single-qubit and two-qubit placeholders that act on all qubits. Each placeholder can be filled with specific gates from a native gate set, which includes predefined selectable quantum gates. This structured approach allows for comprehensive exploration within a manageable framework. The process of assigning specific quantum gates to all placeholders is referred to as sub-sampling. QuantumSupernet utilizes two distinct sub-sampling strategies: random sampling and a genetic algorithm-based search strategy. QuantumSupernet employs a shared parameter-based evaluation strategy to assess the performance of sampled sub-circuits. This method significantly accelerates the QAS process by allowing for the rapid evaluation of multiple sub-circuits without training parameters from scratch.

The QuantumSupernet workflow consists of four main phases. The first is the initialization phase, which defines the supernet structure and native gate set. The second phase is the shared parameter training phase, QuantumSupernet iteratively samples sub-circuits and assesses their performance using corresponding shared parameters, updating the shared parameter pool accordingly. Next is high-performance ansatzs search phase, A search strategy is employed to sample multiple sub-circuits, and their predicted performance is evaluated based on the shared parameter pool. This process outputs the

sub-circuit with the highest predicted performance. The last is the output phase, the selected sub-circuit is trained from scratch to evaluate its actual performance, providing a final assessment of its efficacy.

### 2.1.2 DQAS

Differentiable Quantum Architecture Search (DQAS), proposed by Zhang et al., is the first to introduce a differentiable search model to accelerate the QAS algorithm [24]. We introduce the DQAS algorithm by focusing on three key aspects. Unlike QuantumSupernet, DQAS allows quantum gates to act on arbitrary qubits rather than strictly constraining their arrangement. DQAS employs a differentiable search strategy to sample multiple quantum gate operations, which are then used to construct complete quantum circuits. Specifically, DQAS utilizes a probability model, denoted as  $P(\alpha)$ , to guide the search process. This model transforms the discrete task of searching for quantum circuit architectures into a continuous optimization problem by adjusting the parameters of the probability model through gradient descent techniques. Similar to QuantumSupernet, DQAS adopts a shared parameter-based evaluation strategy to assess the performance of sampled circuits. This approach allows for the efficient evaluation of multiple circuit configurations without the need to train each circuit’s parameters from scratch, thereby reducing computational overhead.

The DQAS workflow consists of four main phases. In the initialization phase, defining the native gate set and the number of gates in the quantum circuit, setting the parameters for the search space. DQAS iteratively samples quantum circuits using the probability model and assesses their performance using shared parameters. This sampling process explores the search space by generating diverse circuit based on the current probability distribution. In the training phase, the performance of the sampled circuits is used to update both the shared parameter pool and the probability model through gradient descent. This phase iteratively refines the search strategy by adjusting the probability model to favor higher-performing circuit configurations. Last, in the output phase, Once the termination condition is met, the final circuit is trained from scratch to evaluate its actual performance. This trained circuit serves as the final output of the algorithm.

## 2.2 Numerical Simulation Tasks

VQAs play a crucial role in quantum computing, offering a wide range of important applications. In QAS, three representative tasks are commonly used as benchmarks to validate the effectiveness of QAS algorithms: ground state energy estimation for molecular systems, solving the MaxCut problem, and classification tasks.

### 2.2.1 Variational Quantum Eigensolver

Calculating the ground state and the lowest energy of Hamiltonian is a fundamental problem in physics research [38–40]. In quantum systems, the Hamiltonian’s dimensionality increases exponentially with the size of system, making it extremely difficult to address the problem. Therefore, researchers have employed the Variational Quantum Eigensolver (VQE), which offers exponential speedup, to address this issue [41–44]. The key to solving this problem is to prepare the ground state  $|\varphi_0\rangle$  of the Hamiltonian  $H$  and compute the lowest energy  $E_0$ , as expressed in (1):

$$E_0 = \frac{\langle \varphi_0^* | H | \varphi_0 \rangle}{\langle \varphi_0^* | \varphi_0 \rangle} \quad (1)$$

Since the  $|\varphi_0\rangle$  is difficult to prepare, VQE approximates it by constructing a states  $|\varphi^n\rangle$  by a PQC  $U(\theta)$ , as shown in (2):

$$|\varphi^n\rangle = U(\theta)|0^n\rangle \quad (2)$$

Here,  $|0^n\rangle$  represents the all-zero quantum state, which often serves as the initial state is and processed by the  $U(\theta)$ . The goal of VQE is to iteratively adjust the parameters  $\theta$  so that  $|\varphi^n\rangle$  gradually approaches  $|\varphi_0\rangle$ . Therefore, calculating the ground state and the lowest energy can be transformed into finding a suitable  $\theta$  that minimizes (3):

$$\theta^* = \arg \min_{\theta} L(\theta) = \langle 0^n | U^\dagger(\theta) H U(\theta) | 0^n \rangle \quad (3)$$

In conclusion, The process of VQE can be summarized as first preparing the quantum state  $|\varphi^n\rangle$  through  $U(\theta)$ , then measuring the energy  $E$  of the state  $|\varphi^n\rangle$ , last update  $\theta$  until the minimum  $E$  is obtained.

### 2.2.2 Variational Quantum Algorithm for the MaxCut Problem

The MaxCut problem is a classic combinatorial optimization problem. Given a graph  $G = (V, E)$ , the objective is to partition its nodes into two distinct sets to maximize the number of edges connecting these sets. The objective function of MaxCut can then be written as:

$$C(z) = \frac{1}{2} \sum_{(i,j) \in E} (1 - z_i z_j) \quad (4)$$

where  $z_i, z_j \in \{+1, -1\}$  and  $z_i$  represents the subset to which vertex  $i$  belongs. The Quantum Approximate Optimization Algorithm (QAOA) is commonly applied to address the MaxCut problem by utilizing alternating optimization to approximate the optimal solution, offering the potential for quantum speedup [1]. In the context of QAOA, the problem Hamiltonian  $H_c$  that encodes the MaxCut objective can be expressed as:

$$H_C = \frac{1}{2} \sum_{(i,j) \in E} (I - Z_i Z_j) \quad (5)$$

where  $Z_i$  and  $Z_j$  are Pauli-Z operators acting on qubits corresponding to the nodes  $i$  and  $j$  of edge  $(i, j) \in G$ . These operators are used to encode the connectivity of the graph in the quantum circuit. The PQC of QAOA is driven by the problem. By adjusting PQC's parameters, QAOA can progressively approximate the optimal solution. In this paper, we utilize a VQA searched by the QAS algorithm to replace ansatz of QAOA for solving the MaxCut problem. The solving process is similar to VQE, except for the Hamiltonian  $H$ .

### 2.2.3 Quantum Neural Network for quantum state classification

Quantum Machine Learning (QML) is an advanced field that integrates quantum computing with machine learning, which aims to leverage the unique properties of quantum mechanics to enhance data analysis efficiency. In this study, we employ a Quantum Neural Network (QNN) to address a binary quantum state classification problem. We utilize the quantum entanglement dataset provided in Ref. [46], which consists of quantum states characterized by different levels of Concurrence Entropy (CE). This dataset is utilized for training the QNN, which comprises an embedding layer, PQC, and a measurement layer. The embedding layer is implemented by using angle encoding with RX rotation gates to map classical information to quantum states. The PQC component, searched by the QAS algorithm, processes the quantum states that contain the information from the dataset. Finally, the measurement layer measures the quantum states through Pauli-Z measurements to obtain classical bits, which are then processed by a multilayer perceptron (MLP) to provide the binary classification result.

## 3 method

### 3.1 TD-QAS Framework

Standard QAS algorithms explore a vast search space that encompasses both circuit topology information (e.g., qubit involvement) and gate-type information. For instance, a fundamental element of a quantum circuit, such as  $[R_x - 0]$ , specifies that the  $R_x$  gate acts on qubit 0. Consequently, an entire circuit can be represented as a sequence of these elements, such as  $[R_x - 0, R_z - 2, YY - 0, XX - 1, R_y - 1, ZZ - 0, R_z - 2]$ , as illustrated in Figure 1 (a). However, this approach significantly amplifies the search difficulty of QAS. Specifically, heuristic search strategies and evaluation mechanisms must concurrently explore and optimize both topology and gate-type information within an extremely large search space, leading to substantial computational complexity and inefficiency. NAS has demonstrated that high-performance CNNs remain largely unaffected by the random replacement of specific operations [45]. If a similar phenomenon could be observed in QAS, separating the search for topology and gate-types would still

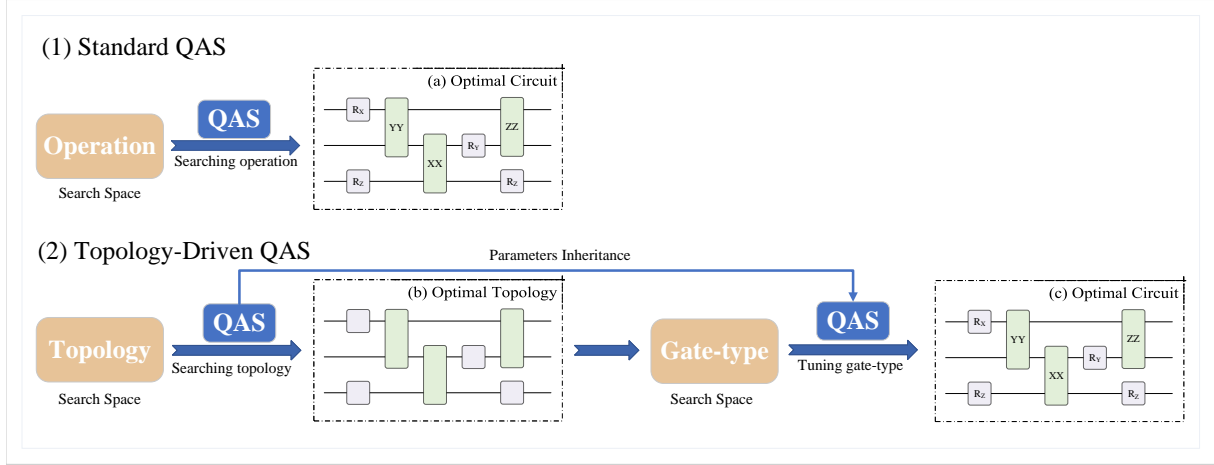


Figure 1 Comparison of Standard QAS and Topology-Driven QAS Framework.

enable the discovery of high-performance quantum circuits. This method can significantly reduce the search space by eliminating the need to search for gate configurations within low-performance topologies.

Through extensive numerical simulations, as discussed in Section 4.1, we found that high-performance quantum circuits exhibit only slight performance changes when quantum gate types are randomly replaced, provided that the circuit topology remains unchanged. This observation suggests that the key to searching for a high-performance VQA lies in determining an optimal circuit topology, followed by the selection of gate types. Therefore, we introduce the Topology-Driven Quantum Architecture Search (TD-QAS) framework, as illustrated in Figure 1 (b), which significantly reduces the search space size. Our framework first employs a topology-driven (TD) phase, which focuses on identifying high-performance topologies while keeping gate types fixed. Subsequently, the framework utilizes a gate tuning (GT) phase to adjust more suitable gate types to enhance circuit performance. To circumvent the substantial computational complexity associated with training the QAS of tuning phase from scratch, the tuning phase inherits parameters from the TD-QAS phase, enabling rapid convergence with only a few additional training epochs.

### 3.2 Implementation of TD-QAS Framework

To realize the TD-QAS framework, we define a topology representation that constructs a dedicated topology search space and establish an evaluation strategy tailored specifically for topology. In our framework, topology is defined by two types of placeholders: single placeholders and double placeholders. These placeholders represent the connectivity and arrangement of gate within the quantum circuit. As illustrated in Figure 1(b), a topology can be represented as  $[single-0, single-2, double-0, double-1, single-1, double-0, single-2]$ . The simplest method to represent topology employs a single placeholder, allowing any type of quantum gate at a given position. However, this approach is insufficient for accurately expressing topology. Moreover, we do not design a three-qubit placeholder or higher, as most QAS methods predominantly focus on single and double -qubit gates. Based on these considerations, defining two types of placeholders is both practical and effective.

To facilitate the search for topology, it is essential to establish an evaluation method specific to topology. The most straightforward approach to evaluate a topology's performance would involve exhaustively enumerating or randomly generating a large number of quantum circuits and using their performance metrics as proxies for the topology's effectiveness. However, this method is computationally prohibitive, especially as the size of the search space grows. We introduce a resource-efficient evaluation strategy termed the Topology Instantiation Evaluation Method. Specifically, we create a topology instance by replacing single and double placeholders with predesignated single-qubit gates (such as  $R_X$ ) and double-qubit gates (such as  $XX$  or  $CNOT$ ). The performance of this topology instance serves as an approximation of the topology's performance. Given that gate types have a relatively limited impact on the performance of high-performance circuits within QAS, this method provides a reasonable and efficient solution to evaluate topology without incurring substantial computational complexity. In our numerical simulations, the topology is directly represented as a specific topology instance. Section 4.2 will verify the accuracy

of the topology instantiation evaluation method in reflecting the true performance of the topology. This validation ensures that our evaluation strategy reliably estimates the effectiveness of different topologies, thereby supporting the efficiency gains of the TD-QAS framework.

### 3.3 Reduction of Search Space

In this subsection, we analyze how the TD-QAS framework effectively reduces the search space, providing an intuitive understanding of its impact. First, the topology search space is primarily determined by the number of placeholder types. The gate-type search space is determined by the searched topology and the number of quantum gates available, which typically defined by manual design or hardware constraints. Given that the number of selectable quantum gates is usually limited, it is feasible to exhaustively enumerate all possible quantum circuits within the gate-type search space for small-scale problems.

To illustrate the efficacy of the TD-QAS framework in reducing the search space, consider a three-qubit quantum circuit consisting of seven quantum gates ( $N_{\text{qubit}} = 3$ ,  $N_{\text{layer}} = 7$ ) with ring connectivity among all qubits. Due to the ring connectivity, there are  $N_{\text{qubit}}$  possible positions for placing either single-qubit and two-qubit gates. Suppose we define  $N_{\text{single}} = 3$  for the single-qubit gates set  $\{R_x, R_y, R_z\}$  and  $N_{\text{double}} = 3$  for the two-qubit gates set  $\{XX, YY, ZZ\}$ . In classical QAS, the number of possible operations per layer is 18 ( $N_{\text{qubit}} \cdot (N_{\text{single}} + N_{\text{double}})$ ), and the search space size is  $18^7$  ( $[N_{\text{qubit}} \cdot (N_{\text{single}} + N_{\text{double}})]^{N_{\text{layer}}}$ ). the TD-QAS framework employs two types of placeholders, placeholders of each layer have 6 ( $2 \cdot N_{\text{qubit}}$ ) possible combination. Thus, the topology search space size becomes  $6^7$  ( $(N_{\text{qubit}} \cdot 2)^{N_{\text{layer}}}$ ). The gate-type search space is  $3^7$  ( $|N_{\text{single}}^x \cdot N_{\text{double}}^{7-x}|$ ), where  $x$  represents the number of single placeholder in the topology. The TD-QAS framework decouples the operation search space into a topology search space and a gate-type search space, reducing it from  $18^7$  to  $6^7$  and  $3^7$ , the corresponding search space reduction ratio is nearly  $2 \times 10^3$ , which calculation formula is (6). In this paper, we use reduction ratio to evaluate the compression efficiency of our framework.

$$\text{Reduction Ratio} = \frac{S_{\text{proposed}}}{S_{\text{traditional}}} \quad (6)$$

### 3.4 Quantum Computational Costs

In this work, we introduce the TD-QAS framework, which is characterized by exceptionally low computational complexity. For QAS, the foremost consideration is quantum computational complexity. Consequently, we utilize quantum computational costs to evaluate the computational overhead of QAS algorithms [35]. Quantum computational costs quantify the estimated time required to execute all quantum circuits generated by QAS algorithms on actual devices. The execution time  $T$  for an individual quantum circuit can be expressed as:

$$T = T_p + (\text{circuit depth}) \cdot T_G + T_M \quad (7)$$

$T_p$  is the time to prepare the initial state,  $T_g$  is the average duration of a quantum gate, and  $T_M$  is the time needed to measure the qubits. where  $T_p + T_M$  is 1 microsecond, and the average gate time  $T_G$  is set to 0.01 microseconds. Circuit depth refers to the maximum length of the directed path from input to output in the quantum circuit, which is directly related to the coherence time required to complete the algorithm. In our numerical simulations, we will compare the quantum computational costs between TD-QAS framework and original QAS algorithms, aiming to evaluate their respective efficiencies.

## 4 Numerical Simulation

In this section, we conduct a comprehensive set of numerical simulations to evaluate the proposed TD-QAS framework across three representative tasks: estimation of ground state energies for molecular systems, solving the MaxCut problem on 100 Erdős-Rényi (ER) graphs, and performing an 8-qubit quantum state classification task.

We first validated that high-performance quantum circuits are only slightly affected in performance when quantum gate types are randomly replaced while maintaining the circuit topology. This indicates that prioritizing the search for circuit topology before fine-tuning gate types is a reasonable approach. Secondly, we validated that the topology instantiation evaluation method can accurately assess circuit topology performance, offering an evaluation strategy that enables QAS algorithms to efficiently search

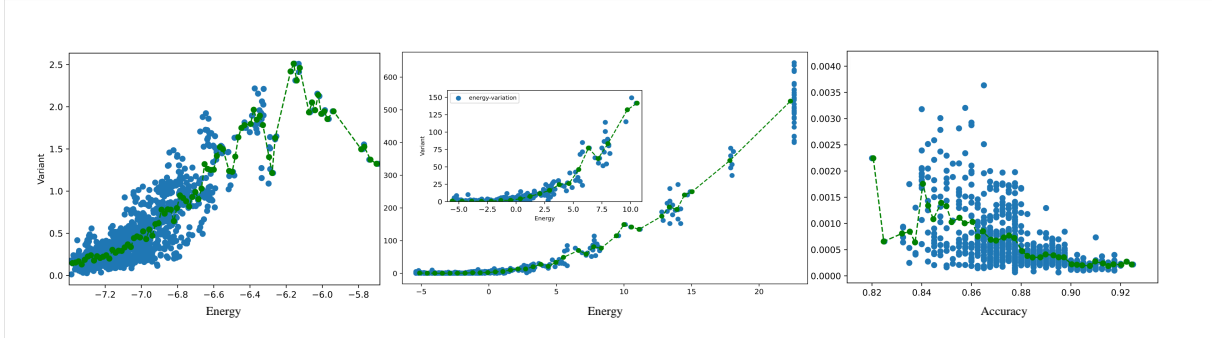


**Figure 2** Simulation results for the three tasks: (a) VQE for ground state energy estimation, (b) VQA for MaxCut problem on Erdős-Rényi(ER) graphs, and (c) QNN for 8-qubit quantum state classification. The horizontal axis represents the original circuit’s performance  $p_i$ , and the vertical axis represents the performance difference  $d_i$ . Blue dots show individual performance differences between original circuits and their variants, while the green line indicates the mean difference across different performance levels.

for circuit topologies with low complexity. Lastly, we verify the superiority of our TD-QAS framework by integrating it with two representative QAS algorithms: QuantumSupernet [23] and DQAS [24]. Our results show that the TD-QAS framework enhances QAS algorithms by identifying higher-performance quantum circuits with lower computational complexity compared to their standard counterparts. Furthermore, we verified that the TD-QAS framework can be easily deployed within existing QAS algorithms, highlighting its versatility and potential to advance the scalability of QAS methodologies.

#### 4.1 Core Hypothesis of TD-QAS: Topology Dominates the Performance of Circuit

The purpose of this section is to validate the core hypothesis of the TD-QAS framework, which posits that quantum circuit topology plays a dominant role over the type of quantum gates in determining VQA performance. This hypothesis is based on our preliminary observations, which suggest that for high-performing circuits, keeping the topology fixed while randomly modifying the quantum gate-type does not significantly impact overall performance. To verify the generality of this phenomenon, we conducted a series of numerical simulations across three different tasks.

We first randomly generated 1,000 original quantum circuits for three distinct tasks. Each quantum circuit consisted of either 30, 35, or 50 quantum gates chosen from the native gate set  $\{H, R_x, R_y, R_z, XX, YY, ZZ\}$ , with qubit connectivity arranged in a ring connectivity. For each original circuit, we created 10 variants by modifying the gate-type. Specifically, we selected one-fifth of the gates in the circuit and replaced them with other gates of the same type (i.e., single-qubit gates replaced by other single-qubit gates), which ensured that the topology remained unchanged. An original-variant set was constructed to verify whether the variants of a high-performance original circuit exhibit reduced performance. After generating these original-variant pairs, each circuit was initialized with parameters five times and trained until convergence. We then selected the best performance from the five training runs as the true performance. This procedure produced data pairs consisting of the original circuit performance and the corresponding performance of its variants  $[p_i, v_i^j]$ , where  $i$  represents the original circuit ( $i \in [1, 1000]$ ) and  $j$  represents the variant circuit ( $j \in [1, 10]$ ). To quantify the performance differences between each original circuit and its variants, we computed the mean squared error (MSE) between them, yielding pairs of original performance and performance difference  $[p_i, d_i]$  as defined:

$$d_i = \frac{1}{n} \sum_{j=1}^n (p_i - p_i^j)^2 \quad i \in [1, 500], j \in [1, 10] \quad (8)$$

These data were plotted as blue dots in Figure 2. To further illustrate the differences at varying performance levels, the range of  $p_i$  was divided into multiple intervals (100, 100, and 50 intervals respectively), and the average  $d_i$  for each interval was calculated and represented by the green line.

The results from Figure 2 show a consistent trend: as the performance of the original circuit improves, the influence of gate modifications on overall performance diminishes. This trend was consistently observed across all three tasks, highlighting the generality and robustness of our findings. These results strongly support the core hypothesis of the TD-QAS framework.

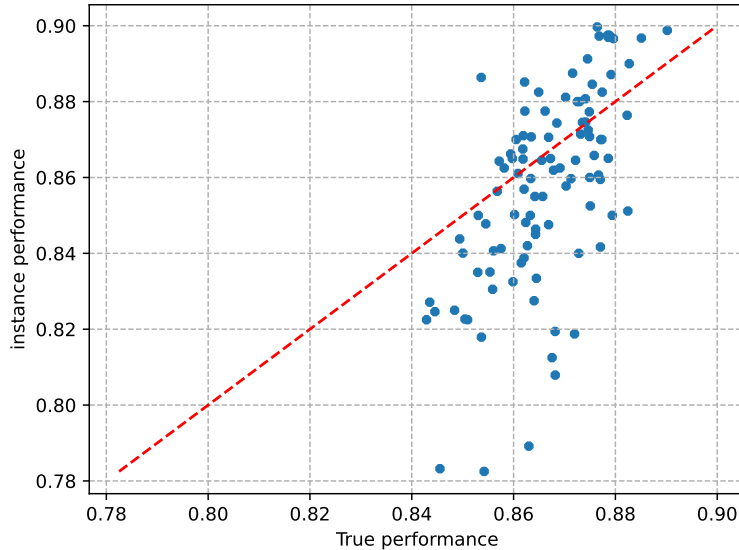


**Figure 3** Correlation of true performance and instance performance on the state classification task.

## 4.2 Topology Instantiation Evaluation Method

The TD-QAS framework proposes that QAS should first search for topology. However, existing QAS methods lack a dedicated method for evaluating topology. The most straightforward way to evaluate a topology’s performance is to exhaustively assess all potential quantum circuits or a large number of circuits and then use their average performance as a proxy for the topology’s performance. Unfortunately, this approach is impractical due to its high complexity. As observed in Section 4.1, we find that random gate substitutions have minimal impact on performance for high-performance circuits. Therefore, we propose a highly resource-efficient evaluation strategy called the topology instantiation evaluation method. This method represents the topology using topology instances, which replace the corresponding placeholders with specific quantum gates. To verify the effectiveness of this method, we calculated the correlation between the approximate true performance and the instance performance calculated by our method.

We first generated 100 circuit topologies. For each topology, we generated 100 quantum circuits by randomly selecting quantum gates from the set  $\{H, R_x, R_y, R_z, XX, YY, ZZ\}$ , arranged in a ring connectivity. We then calculated the performance obtained from two evaluation methods. For each topology, we initialized the parameters for the corresponding 100 circuits and trained them to obtain their average performance, which served as the approximate true performance, denoted as  $y$ . In our proposed method, we replaced the single-qubit and two-qubit placeholders with  $R_x$  gates and  $XX$  gates, respectively, generating one instance for each topology. Similarly, we calculated the performance of these instances, denoted as  $y'$ . Finally, we calculated the Pearson correlation coefficient between the true performance,  $y$ , and the instance performance,  $y'$ , as defined in (9):

$$r = \frac{\sum (y_i - \bar{y})(y'_i - \bar{y}')}{\sqrt{\sum (y_i - \bar{y})^2 \cdot \sum (y'_i - \bar{y}')^2}} \quad (9)$$

The numerical simulation results indicated correlation values of 0.68, 0.59, and 0.62 for the three tasks. We present the results for one task in Figure 3. For comparison, the widely used performance predictor achieved a correlation of 0.71 [25], while it required extensive complexity to prepare training datasets. Thus, our method can provide a reasonably accurate assessment of topology’s performance with low complexity.

## 4.3 TD-QAS framework

In the previous sections, we discussed the challenges faced by existing QAS algorithms, including the vast search spaces that often lead to local optima and excessive quantum computational costs. To tackle

these challenges, we propose the TD-QAS framework, which aims to enhance the efficiency of QAS by decomposing the operational search space into separate topology and gate-type search spaces. To thoroughly assess the effectiveness of the TD-QAS framework, we compare several metrics from both the TD and GT phases with those of standard QAS algorithms. These metrics include the size of the search space, performance in specific tasks, circuit properties, and overall quantum computational costs. In the following subsections, we apply the TD-QAS framework to two representative QAS algorithms and analyze their performance.

#### 4.3.1 TD-QuantumSupernet framework

In this section, we use QuantumSupernet to implement the TD-QAS framework, followed by a series of numerical simulations. The core algorithm of QuantumSupernet is described in Section 2.1.1. Therefore, we will first explain how to implement the TD and GT phases using QuantumSupernet. Next, we define the hyperparameters for various numerical simulation tasks, highlighting their impact on the comparison variables. Finally, we execute the algorithm using these hyperparameters and analyze the results of the numerical simulations. For the simulations, we select the same VQE and classification tasks used in QuantumSupernet.

**Overview of Framework** In this section, we provide an overview of the implementation process of the TD-QAS framework using QuantumSupernet. The TD phase begins by defining the topology search space, which is determined by the structure of the supernet and the native gate set. The number of qubits ( $N_{\text{qubit}}$ ) and the number of layers ( $N_{\text{layer}}$ ) are specified by the task. Additionally, the native gate set is set to  $R_x, I, CNOT, CI$ , where  $CI$  refers to the Controlled-Identity Gate. If a sampled topology instance contains an  $I$  or  $CI$  gate at a specific location, it indicates that no quantum gate will be placed at that position, and the GT phase will skip fine-tuning for that location. Next, a randomly searching algorithm is exploring potential high-performance topologies. The performance of each topology instance is evaluated using shared parameters, with feedback used to update these parameters. Specifically, we use  $N_{\text{experts}}$  shared parameters to assess the performance of each topology, which allows for more accurate performance evaluations. The shared parameters are trained over  $N_{\text{train}}$  iterations. During the first  $T_{\text{warm}}$  iterations, a randomly selected expert from the  $N_{\text{experts}}$  pool evaluates the topology instances and updates the optimal shared parameters. After the warm-up phase, all  $N_{\text{experts}}$  participate in the evaluation, but only the shared parameters with the best performance are updated. After the convergence of shared parameters, we evaluate  $N_{\text{search}}$  topology instances and select the most optimal topology. In the GT phase, the gate-type search space consists of the previously identified topology and the native gate set  $A_g$ . The shared parameters for the GT phase are inherited from the TD phase. This inheritance mechanism involves replicating the shared parameters from the TD phase based on the number of single-qubit and two-qubit gates available in the native gate pool. To enhance the accuracy of the evaluation, we perform additional training on the inherited parameters for a few extra iterations, denoted as  $T_{\text{extra}}$ , which further refines the assessment of specific circuit performances.

With the designed hyperparameters, we calculate the comparison variables, including the search space size and the total quantum computational cost (QCC). Since the supernet consistently applies both single-qubit and two-qubit gates to every qubit, the original search space is calculated as  $(|A[\text{single}]|^{N_{\text{qubit}}} \cdot |A[\text{double}]|^{N_{\text{qubit}}})^{N_{\text{layer}}}$ , where  $|A[\text{single}]|$  denotes the number of single-qubit gates in the native gate set. The topology and gate-type search space is then defined as  $(2^{N_{\text{qubit}}})^{N_{\text{layer}}}$  and  $|A[\text{single}]|^{N_{\text{layer}}-x} \cdot |A[\text{double}]|^x$ , where  $2^{N_{\text{qubit}}}$  represents the combinations of single and double placeholder gates across different qubits, and  $x$  is the number of double placeholder gates in the searched topology. The quantum computational cost (QCC) for QuantumSupernet and the TD phase is given by  $\sum_1^{T_{\text{warm}}} T_i + \sum_{T_{\text{warm}}}^T T_i * N_{\text{experts}} + \sum_1^{N_{\text{search}}} T_i * N_{\text{experts}}$ . The QCC for the GT phase is given by  $\sum_1^{N_{\text{search}}} T_i \cdot (1 + T_{\text{extra}})$ . Each circuit of quantum computational costs  $T_i$  is defined as (7).

**Numerical Simulation on the VQE Task** In this section, we evaluate the performance of the TD-QAS framework through numerical simulations. We first replicate the ground state energy estimation task for a 4-qubit hydrogen molecule, which is consistent with the simulation in Ref. [23]. While this small-scale task provides valuable insight, it does not fully showcase the potential of the TD-QAS framework. Therefore, we extend the validation to larger tasks, including the 5-qubit Heisenberg model.

**Table 1** Simulation Results for the Ground State Energy Estimation of Hydrogen. The "Property" column shows the layer depth, number of parameterized gates, and total gate count of the searched circuits. "QuantumSupernet-5" and "TD-1" refer to the method with  $N_{\text{experts}}$  as indicated.

Method	Energy	Property	QCC	Scenario
QuantumSupernet-5	-1.13610	6.2, 9.2, 16.1	4471.4	noiseless
TD-1	-1.13572	4.6, 3.0, 7.3	846.2	noiseless
GT-1	-1.13572	4.6, 3.0, 7.3	16.7	noiseless
QuantumSupernet-5	-0.97079	3.8, 7.4, 12.8	4327.4	noise
TDGT-1	-1.09169	4.0, 3.0, 6.4	841.6	noise

For the simulation task involving the estimation of the ground state energy of hydrogen (which has a ground state energy of -1.13618 Hartree), the construction of the Hamiltonian is detailed in QuantumSupernet [23]. Before performing the numerical simulations, we define the hyperparameters and compare the search space sizes of the QuantumSupernet and TD-QAS methods. Specifically, the number of qubits ( $N_{\text{qubit}}$ ) is set by to 4 and the number of layers ( $N_{\text{layer}}$ ) is to 3. For the QuantumSupernet, the native gate set  $A$  is defined as  $\{I, R_y, R_z, CNOT, CI\}$ . In the TD-QAS framework, the gate sets are defined as  $A_t = \{R_y, I, CNOT, CI\}$  for the topology-driven phase and  $A_g = \{R_y, R_z, CNOT\}$  for the gate tuning phase. Under these settings, the search space for the QuantumSupernet is calculated as  $(3^4 \cdot 2^4)^3$ . The search space for the TD phase is calculated as  $(2^4 \cdot 2^4)^3$ , while the GT phase operates within a search space ranging from 1 to  $2^{12}$ . This decoupling results in a search space reduction ratio of  $2.5 \times 10^1$ . Due to the reduced search space, we use smaller values for the number of experts ( $N_{\text{experts}}$ ) and the total number of iterations ( $T$ ) to enhance efficiency. Specifically, for the QuantumSupernet, we set  $N_{\text{experts}} = 5$ ,  $T = 500$ ,  $T_{\text{warm}} = 200$ , and  $N_{\text{search}} = 500$ . In the TD phase, these parameters are adjusted to  $N_{\text{experts}} = 1$ ,  $T = 200$ ,  $T_{\text{warm}} = 100$ , and  $N_{\text{search}} = 500$ . In the GT phase, we set  $T_{\text{extra}} = 1$ . Given the small problem size and native gate set, an exhaustive search is feasible, and thus  $N_{\text{search}}$  is omitted in the GT phase.

A comparison of the numerical simulations for these methods is presented in Table 1. In the noiseless scenario, the quantum circuit obtained in the TD and GT phases performs comparably to the QuantumSupernet. However, the circuit depth is reduced to 74.1%, the number of parameterized gates to 32.6%, and the total number of gates to 45.3% of the QuantumSupernet. As a result, the quantum computational cost is reduced to approximately 19% of the QuantumSupernet. This demonstrates the effectiveness of independently searching for the topology and gate types, with the task being successfully completed by the topology search alone, achieving chemical accuracy with an estimation error of less than 0.0016 Hartree. In the noisy scenario, the TD-QAS framework identifies higher-performance circuits, likely due to the reduced circuit depth. Overall, the results from both noiseless and noisy scenarios confirm that prioritizing the search for circuit topology, followed by fine-tuning the gate types, enables the TD-QAS framework to find high-performance circuits with lower quantum computational costs.

To further demonstrate the capabilities of the TD-QAS framework for larger-scale problems, we applied it to the ground state energy estimation of the 5-qubit Heisenberg model. The Hamiltonian for the Heisenberg model is defined as  $\sum_{i=1}^n (X_i X_{i+1} + Y_i Y_{i+1} + Z_i Z_{i+1}) + \sum_{i=1}^n Z_i$ , and the ground state energy is -8.47213. The hyperparameters for this simulation are defined as follows:  $N_{\text{qubit}}=5$ ,  $N_{\text{layer}}=6$ ,  $A=\{I, R_x, R_y, R_z, CNOT, CI\}$ ,  $A_t=\{R_y, I, CNOT, CI\}$ , and  $A_g=\{R_x, R_y, R_z, CNOT\}$ . With these settings, the search space for the QuantumSupernet is calculated as  $(4^5 \cdot 2^5)^6 = 2^{80}$ , while the search space for the TD and GT phases is  $2^{60}$  and  $1 \sim 3^{30}$ , respectively. This results in a search space reduction ratio of approximately  $1 \times 10^7$ . To evaluate the performance of the TD-QAS framework and compare it to the QuantumSupernet, we executed simulations with different values of  $N_{\text{experts}}$ . Specifically, we set  $N_{\text{experts}} = 1$  and  $N_{\text{experts}} = 5$ . The hyperparameters for the QuantumSupernet are  $T = 500$ ,  $T_{\text{warm}} = 200$ , and  $N_{\text{search}} = 500$ . For the TD-QAS framework, the parameters are adjusted as follows:  $T = 200$ ,  $T_{\text{warm}} = 100$ , and  $N_{\text{search}} = 300$ . In the GT phase, we set  $T_{\text{extra}} = 1$  and  $N_{\text{search}} = 100$ .

The results of the numerical simulations are presented in Table 2. With the same  $N_{\text{experts}}$ , the TD and GT methods outperform the QuantumSupernet. This suggests that the TD-QAS framework enhances the performance of the QuantumSupernet by efficiently reducing circuit complexity. When comparing simulations with different numbers of experts ( $N_{\text{experts}} = 1$  and  $N_{\text{experts}} = 5$ ), we observe that the QuantumSupernet shows a higher dependency on  $N_{\text{experts}}$ . This is likely due to the larger number of parameterized quantum gates in the circuits searched by QuantumSupernet, which results in greater sensitivity to the number of experts. In contrast, the circuits found by the TD and GT methods have fewer parameters, leading to more stable performance across varying values of  $N_{\text{experts}}$ . This highlights

**Table 2** Simulation Results for the Ground State Energy Estimation of Heisenberg. The property presents layer depth, number of parameterized Gates, and total gate number of searched circuits. QuantumSupernet-5 and TD-1 present method- $N_{\text{experts}}$ 

Method	Energy	Property	QCC	Scenario
QuantumSupernet-1	-7.64036	16.0,38.2,51.6	1155.1	noiseless
TD-1	-8.00899	14.8,18.4,32.6	624.4	noiseless
GT-1	-8.11899	14.8,18.4,32.6	332.6	noiseless
QuantumSupernet-5	-8.22164	16.6,38.4,52.8	4873.2	noiseless
TD-5	-8.01173	15.4,21.0,37.4	3945.2	noiseless
GT-5	-8.14162	15.4,21.0,37.4	2126.9	noiseless
QuantumSupernet-5	-7.82812	15.1,36.7,50.2	4893.2	noise
TDGT-1	-8.02160	12.5,20.5,34.0	997.5	noise

**Table 3** Numerical Simulation Results for State Classification Task. The property presents layer depth, number of parameterized Gates, and total gate number of searched circuits. QuantumSupernet-5 and TD-1 present method- $N_{\text{experts}}$ 

Method	Success Rate	Property	QCC	Scenario
QuantumSupernet-5	0.83917	14.3 , 44.3 , 62.8	4800.6	noiseless
TD-1	0.84250	15.0 , 28.7 , 49.7	620.1	noiseless
GT-1	0.85017	15.0 , 28.7 , 49.7	224.9	noiseless
QuantumSupernet-5	0.80064	14.1 , 42.4 , 58.7	4792.2	noise
TDGT-1	0.81554	14.8 , 24.1 , 42.3	927.4	noise

the TD-QAS framework’s ability to reduce the training burden and, consequently, the QCC. Additionally, the circuits discovered in both the TD and GT phases exist within the operation search space, but were not identified by the QuantumSupernet. This suggests that the TD-QAS framework may help mitigate the risk of the QAS algorithm getting trapped in local optima, thereby facilitating the discovery of more optimal quantum circuits.

**QNN for State Classification Task** To assess the performance improvements of the TD-QAS framework on more complex tasks, we conducted a numerical evaluation using an 8-qubit quantum state classification task. Specifically, we employed a QNN to address a binary classification problem, where the input consisted of quantum states with varying levels of entanglement, characterized by Concurrence Entropy ( $CE = 0.15$  and  $CE = 0.45$ ). The quantum dataset used in this experiment is based on the dataset from Ref. [46].

The hyperparameter settings for the numerical simulation are detailed in follow,  $N_{\text{qubit}}=8$ ,  $N_{\text{layer}}= 6$ ,  $A=\{I, R_x, R_y, R_z, CNOT, CI\}$ ,  $A_t=\{R_y, I, CNOT, CI\}$ , and  $A_g=\{R_x, R_y, R_z, CNOT\}$ . With these parameters, we calculate that the search space for the QuantumSupernet is  $2^{144}$ , while the search space for the TD and GT phases is  $2^{96}$  and  $1 \sim 3^{30}$ , respectively. This results in a search space reduction ratio of approximately  $2.6 \times 10^6$ . The simulation hyperparameters for the QuantumSupernet are set as  $T = 500$ ,  $T_{\text{warm}} = 200$ , and  $N_{\text{search}} = 500$ . For the TD-QAS framework, we set  $T = 200$ ,  $T_{\text{warm}} = 100$ , and  $N_{\text{search}} = 300$  in the TD phase, while in the GT phase,  $T_{\text{extra}} = 1$  and  $N_{\text{search}} = 100$ .

Table 3 summarizes the simulation results for the state classification task. The TD-QAS framework successfully identifies higher-performance circuits compared to the QuantumSupernet, all while incurring lower quantum computational costs. Notably, this task involves a much larger search space than any previously examined task, and the TD-QAS framework demonstrates significant improvements in QAS performance compared to earlier Numerical simulations. These results further emphasize the importance of the TD-QAS framework in effectively reducing the search space and improving quantum circuit optimization.

#### 4.3.2 TD-DQAS framework

To validate the generality and effectiveness of the TD-QAS framework across different QAS algorithms, this section implements the TD-QAS framework using the DQAS algorithm and conducts a systematic performance analysis. The core algorithm of DQAS has been detailed in Section 2.1.2. Similar to Section 4.3.1, we first describe the implementation details of the TD-QAS framework using DQAS, followed by an introduction to the hyperparameter settings. Finally, we execute the QAS algorithms and analyze their results.

**Table 4** Numerical Simulation Results for TD-DQAS.

Method	Performance	QCC	Scenario
VQE for TFIM			
DQAS	-6.38688	9972.5	noiseless
TD	-6.53971	2391.4	noiseless
GT	-7.06726	118.7	noiseless
DQAS	-6.12504	10786.5	noise
TDGT	-6.71821	3604.2	noise
VQA for MaxCut			
DQAS	0.77	11917.0	noiseless
TD	0.90	2322.8	noiseless
GT	0.93	361.8	noiseless
DQAS	0.76	13835.9	noise
TDGT	0.89	2945.6	noise
QNN for State Classification			
DQAS	0.78095	10603.4	noiseless
TD	0.78222	1750.7	noiseless
GT	0.85897	280.1	noiseless
DQAS	0.77460	11894.4	noise
TDGT	0.79811	2166.5	noise

**Overview of Framework** In this section, we outline the process of implementing the TD-QAS framework with DQAS. The goal of DQAS is to identify a high-performance quantum circuit that contains  $N_{\text{gate}}$  quantum gates, where arbitrary single-qubit or two-qubit gates can be placed at any position. In the TD phase, the native gate set is defined as  $A_t$  is  $\{R_x, XX\}$ . DQAS uses a probabilistic model to select a batch of  $N_{\text{batch}}$  quantum circuits, each of which is composed of  $N_{\text{gate}}$  gates chosen from the set  $A_t$  and their corresponding qubit positions. The performance of the selected circuits is evaluated using shared parameters, which are then updated using feedback from the quantum circuit evaluation. This process continues until  $N_{\text{train}}$  iterations or until convergence. Finally, the probability model selects the optimal topology instance with the highest probability. DQAS uses mini-batch gradient descent to optimize the model. Generally, models with greater complexity require a larger batch size. In the GT phase, the shared parameters from the TD phase are inherited, and the probability model is trained from scratch. The model fine-tunes the quantum gates from the native gate set based on the searched topology. Since gate placement positions are not considered in this phase, the trainable parameters in the probability model are minimal, allowing for a smaller  $N_{\text{train}}$ .

We calculate and compare several key metrics, including the search space and total quantum computational costs. The search space of DQAS is defined by  $(|A| \cdot N_{\text{qubit}})^{N_{\text{gate}}}$ , whereas the search space of the TD and GT phases is  $(2 \cdot N_{\text{qubit}})^{N_{\text{gate}}}$  and  $|A[\text{single}]|^{N_{\text{gate}}-x} \cdot |A[\text{double}]|^x$ , respectively. The QCC for all methods is computed as  $\sum_{i=1}^{N_{\text{train}}} \sum_{j=1}^{N_{\text{batch}}} T_i^j$ . In this section, we do not compare the properties of the quantum circuits, such as depth and the number of parameterized gates, as the gate placement rules in DQAS allow arbitrary single-qubit gates to act on any position.

**Numerical Simulation of TD-DQAS** This section validates the capacity of the TD-DQAS framework across three tasks: the VQE task, the MaxCut problem, and the state classification task. Since the numerical simulation setup and conclusions largely overlap with those discussed in earlier sections, we focus on presenting a comparative analysis of the results rather than repeating the full details.

For each task, we set the following hyperparameters:  $A = A_g = \{R_x, R_y, R_z, XX, YY, ZZ\}$   $A_t = \{R_x, XX\}$ .  $N_{\text{train}} = 500$ , the  $N_{\text{batch}}$  of DQAS, TD and GT phase is 32, 8, 8, respectively. For the VQE task, we selected the 6-qubit TFIM, using the ground state energy as the performance metric. We set  $N_{\text{qubit}} = 6$  and  $N_{\text{gate}} = 36$ . Therefore, the search space of DQAS, TD and GT phase is  $36^{36}$ ,  $12^{36}$  and  $3^{36}$ . The search space reduction ratio is nearly  $1.5 \times 10^{17}$ . In the MaxCut problem, we used the ER model to randomly generate 100 distinct graphs, each containing 10 nodes, with an edge creation probability set to 0.5. The quantum circuit's output apart from the maximum cut, serves as the performance metric. We set  $N_{\text{qubit}} = 10$ ,  $N_{\text{gate}} = 20$ . Therefore, the search space of DQAS, TD and GT phase is  $60^{20}$ ,  $20^{20}$  and  $3^{20}$ . The search space reduction ratio is nearly  $3.5 \times 10^{10}$ . For the quantum state classification task,

classification accuracy serving as the performance metric. We set  $N_{\text{qubit}} = 8$ ,  $N_{\text{gate}} = 30$ . Therefore, the search space of DQAS, TD, and GT phase is  $48^{30}$ ,  $16^{30}$  and  $3^{30}$ . The search space reduction ratio is nearly  $2 \times 10^{15}$ . The detailed numerical results for each task are presented in Table 4, which shows that the TD-DQAS framework outperforms the DQAS algorithm across all tasks. In both noiseless and noisy scenarios, TD-QAS significantly enhances the performance of QAS algorithms, enabling them to search for higher-performance quantum circuits with lower quantum resource costs.

## 5 Conclusion and Future Work

In this paper, we proposed the TD-QAS framework, which significantly enhances the efficiency and scalability of QAS by decoupling the search process into two key steps: topology searching and gate-type fine-tuning. This novel approach reduces the size and complexity of the search space, allowing for a more resource-efficient exploration. Our experiments across various tasks and scenarios, including both noisy and noiseless scenarios, demonstrate that TD-QAS can effectively discover high-performing PQCs with reduced quantum computational costs. The TD-QAS framework was successfully implemented with two widely used QAS algorithms, i.e., QuantumSupernet and DQAS, demonstrating its compatibility. The numerical results indicate that TD-QAS not only improves QAS capacity but also reduces the risk of convergence to suboptimal circuits.

Under future directions, we first aim to extend TD-QAS to other QAS algorithms, broadening its utility and adaptability. Then we will focus on optimizing the evaluation strategy, such as using a predictor-base evaluation method. Additionally, we plan to explore the scalability of TD-QAS for larger quantum circuits and more complex problem spaces. By refining these aspects, we aim to establish TD-QAS as a foundational approach for efficient and scalable QAS across various quantum computing applications.

**Acknowledgements** This work is supported by National Natural Science Foundation of China (Grant Nos. 62372048, 62371069, 62272056)

## References

- 1 Farhi E, Goldstone J, Gutmann S. A quantum approximate optimization algorithm. arXiv preprint arXiv:1411.4028, 2014.
- 2 Ni X. H., Cai B. B., Liu H. L., et al. Multilevel Leapfrogging Initialization Strategy for Quantum Approximate Optimization Algorithm. *Advanced Quantum Technologies*, 2024, 7(5): 2300419.
- 3 Shor P. W. Polynomial-time algorithms for prime factorization and discrete logarithms on a quantum computer. *SIAM Review*, 1999, 41(2): 303-332.
- 4 Harrow A. W., Hassidim A., Lloyd S. Quantum algorithm for linear systems of equations. *Physical Review Letters*, 2009, 103(15): 150502.
- 5 Peruzzo A., McClean J., Shadbolt P., et al. A variational eigenvalue solver on a photonic quantum processor. *Nature Communications*, 2014, 5(1): 4213.
- 6 Grant E., Benedetti M., Cao S., et al. Hierarchical quantum classifiers. *npj Quantum Information*, 2018, 4(1): 65.
- 7 Havlíček V., Córcoles A. D., Temme K., et al. Supervised learning with quantum-enhanced feature spaces.
- 8 Otterbach J. S., Manenti R., Alidoust N., et al. Unsupervised machine learning on a hybrid quantum computer. arXiv preprint arXiv:1712.05771, 2017.
- 9 Song Y., Wu Y., Wu S., et al. A quantum federated learning framework for classical clients. *Science China Physics, Mechanics & Astronomy*, 2024, 67(5): 250311.
- 10 Shi M., Situ H., Zhang C. Hybrid quantum neural network structures for image multi-classification. *Physica Scripta*, 2024, 99(5): 056012.
- 11 Wu S., Li R., Song Y., et al. Quantum Assisted Hierarchical Fuzzy Neural Network for Image Classification. *IEEE Transactions on Fuzzy Systems*, 2024.
- 12 Chen C., Zhao Q. Quantum generative diffusion model. arXiv preprint arXiv:2401.07039, 2024.
- 13 Preskill J. Quantum computing in the NISQ era and beyond. *Quantum*, 2018, 2: 79.
- 14 Knill E. Quantum computing with realistically noisy devices. *Nature*, 2005, 434(7029): 39-44.
- 15 Situ H., He Z., Wang Y., et al. Quantum generative adversarial network for generating discrete distribution. *Information Sciences*, 2020, 538: 193-208.
- 16 Cong I., Choi S., Lukin M. D. Quantum convolutional neural networks. *Nature Physics*, 2019, 15(12): 1273-1278.
- 17 Cerezo M., Arrasmith A., Babbush R., et al. Variational quantum algorithms. *Nature Reviews Physics*, 2021, 3(9): 625-644.
- 18 Li L., Li J., Song Y., et al. An efficient quantum proactive incremental learning algorithm. *Science China Physics, Mechanics & Astronomy*, 2025, 68(1): 1-9.
- 19 Kandala A., Mezzacapo A., Temme K., et al. Hardware-efficient variational quantum eigensolver for small molecules and quantum magnets. *Nature*, 2017, 549(7671): 242-246.
- 20 Romero J., Babbush R., McClean J. R., et al. Strategies for quantum computing molecular energies using the unitary coupled cluster ansatz. *Quantum Science and Technology*, 2018, 4(1): 014008.
- 21 Kuo E. J., Fang Y. L. L., Chen S. Y. C. Quantum architecture search via deep reinforcement learning. arXiv preprint arXiv:2104.07715, 2021.
- 22 He Z., Deng M., Zheng S., et al. Training-free quantum architecture search. *Proceedings of the AAAI Conference on Artificial Intelligence*, 2024, 38(11): 12430-12438.
- 23 Du Y., Huang T., You S., et al. Quantum circuit architecture search for variational quantum algorithms. *npj Quantum Information*, 2022, 8(1): 62.
- 24 Zhang S. X., Hsieh C. Y., Zhang S., et al. Differentiable quantum architecture search. *Quantum Science and Technology*, 2022, 7(4): 045023.
- 25 Zhang S. X., Hsieh C. Y., Zhang S., et al. Neural predictor based quantum architecture search. *Machine Learning: Science and Technology*, 2021, 2(4): 045027.

- 26 He Z., Wei J., Chen C., et al. Gradient-based optimization for quantum architecture search. *Neural Networks*, 2024, 179: 106508.
- 27 Duong T., Truong S. T., Tam M., et al. Quantum neural architecture search with quantum circuits metric and bayesian optimization. arXiv preprint arXiv:2206.14115, 2022.
- 28 He Z., Li Z., Deng M., et al. Quantum Architecture Search with Neural Predictor Based on Graph Measures. *Advanced Quantum Technologies*, 2400223.
- 29 Situ H., He Z., Zheng S., et al. Distributed quantum architecture search. *Physical Review A*, 2024, 110(2): 022403.
- 30 Zhao T., Chen B., Wu G., et al. Hierarchical Quantum Architecture Search for Variational Quantum Algorithms. *IEEE Transactions on Quantum Engineering*, 2024.
- 31 Martyniuk D., Jung J., Paschke A. Quantum Architecture Search: A Survey. arXiv preprint arXiv:2406.06210, 2024.
- 32 Sun Y., Ma Y., Tresp V. Differentiable quantum architecture search for quantum reinforcement learning. *Proceedings of the 2023 IEEE International Conference on Quantum Computing and Engineering (QCE)*, IEEE, 2023, 2: 15-19.
- 33 Wu W., Yan G., Lu X., et al. Quantumdarts: differentiable quantum architecture search for variational quantum algorithms. *International Conference on Machine Learning*, PMLR, 2023: 37745-37764.
- 34 He Z., Su J., Chen C., et al. Search space pruning for quantum architecture search. *The European Physical Journal Plus*, 2022, 137(4): 491.
- 35 Guerreschi G. G., Matsuura A. Y. QAOA for Max-Cut requires hundreds of qubits for quantum speed-up. *Scientific Reports*, 2019, 9(1): 6903.
- 36 Elsken T., Metzen J. H., Hutter F. Neural architecture search: A survey. *Journal of Machine Learning Research*, 2019, 20(55): 1-21.
- 37 Shu Y., Wang W., Cai S. Understanding architectures learned by cell-based neural architecture search. *Proceedings of the International Conference on Learning Representations (ICLR) 2020*.
- 38 Lolur P., Rahm M., Skogh M., et al. Benchmarking the variational quantum eigensolver through simulation of the ground state energy of prebiotic molecules on high-performance computers. *AIP Conference Proceedings*, 2021, 2362(1): 030005.
- 39 Nakanishi K. M., Mitarai K., Fujii K. Subspace-search variational quantum eigensolver for excited states. *Physical Review Research*, 2019, 1(3): 033062.
- 40 Parrish R. M., Hohenstein E. G., McMahon P. L., et al. Quantum computation of electronic transitions using a variational quantum eigensolver. *Physical Review Letters*, 2019, 122(23): 230401.
- 41 Tilly J., Chen H., Cao S., et al. The variational quantum eigensolver: a review of methods and best practices. *Physics Reports*, 2022, 986: 1-128.
- 42 Wang D., Higgott O., Brierley S. Accelerated variational quantum eigensolver. *Physical Review Letters*, 2019, 122(14): 140504.
- 43 Verteletskyi V., Yen T. C., Izmaylov A. F. Measurement optimization in the variational quantum eigensolver using a minimum clique cover. *The Journal of Chemical Physics*, 2020, 152(12): 124114.
- 44 Huggins W. J., Lee J., Baek U., et al. A non-orthogonal variational quantum eigensolver. *New Journal of Physics*, 2020, 22(7): 073009.
- 45 Wang L., Chen L. Ftso: Effective nas via first topology second operator. arXiv preprint arXiv:2303.12948, 2023.
- 46 Schatzki L., Arrasmith A., Coles P. J., et al. Entangled datasets for quantum machine learning. arXiv preprint arXiv:2109.03400, 2021.